

## RESEARCH ARTICLE

# The astrovirus N-terminal nonstructural protein anchors replication complexes to the perinuclear ER membranes

Hashim Ali<sup>1‡</sup>, David Noyvert<sup>1</sup>, Jacqueline Hankinson<sup>1</sup>, Gemma Lindsey<sup>1</sup>, Aleksei Lulla<sup>2</sup>, Valeria Lulla<sup>1\*</sup>

**1** Department of Pathology, University of Cambridge, Cambridge, United Kingdom, **2** Department of Biochemistry, University of Cambridge, Cambridge, United Kingdom

‡ Current address: Division of Infection and Immunity, University College London, London, United Kingdom  
\* [vl284@cam.ac.uk](mailto:vl284@cam.ac.uk)



## OPEN ACCESS

**Citation:** Ali H, Noyvert D, Hankinson J, Lindsey G, Lulla A, Lulla V (2024) The astrovirus N-terminal nonstructural protein anchors replication complexes to the perinuclear ER membranes. *PLoS Pathog* 20(7): e1011959. <https://doi.org/10.1371/journal.ppat.1011959>

**Editor:** Bert L. Semler, University of California, Irvine, UNITED STATES OF AMERICA

**Received:** January 8, 2024

**Accepted:** June 20, 2024

**Published:** July 15, 2024

**Copyright:** © 2024 Ali et al. This is an open access article distributed under the terms of the [Creative Commons Attribution License](https://creativecommons.org/licenses/by/4.0/), which permits unrestricted use, distribution, and reproduction in any medium, provided the original author and source are credited.

**Data Availability Statement:** The authors confirm that all data underlying the findings are fully available without restriction. All relevant data are within the paper and its [Supporting information](#) files.

**Funding:** This work was funded by a Sir Henry Dale Fellowship (220620/Z/20/Z) from the Wellcome Trust and the Royal Society, an Isaac Newton Trust/Wellcome Trust ISSF/University of Cambridge Joint Research Grant and MRC project grant (MR/T000376/1) to V.L. D.N. is supported by

## Abstract

An essential aspect of positive-sense RNA virus replication is anchoring the replication complex (RC) to cellular membranes. Positive-sense RNA viruses employ diverse strategies, including co-translational membrane targeting through signal peptides and co-opting cellular membrane trafficking components. Often, N-terminal nonstructural proteins play a crucial role in linking the RC to membranes, facilitating the early association of the replication machinery. Astroviruses utilize a polyprotein strategy to synthesize nonstructural proteins, relying on subsequent processing to form replication-competent complexes. This study provides evidence for the perinuclear ER membrane association of RCs in five distinct human astrovirus strains. Using tagged recombinant classical human astrovirus 1 and neurotropic MLB2 strains, we establish that the N-terminal domain guides the ER membrane association. We identified di-arginine motifs responsible for the perinuclear ER retention and formation of functional RCs through mutational analysis of the N-terminal domain in replicon and reverse genetics systems. In addition, we demonstrate the association of key components of the astrovirus replication complex: double-stranded RNA, RNA-dependent RNA polymerase, protease, and N-terminal protein. Our findings highlight the intricate virus-ER interaction mechanism employed by astroviruses, potentially leading to the development of novel antiviral intervention strategies.

## Author summary

Human astroviruses are a significant cause of acute gastroenteritis, accounting for up to 9% of cases in young children. Immunocompromised individuals and infants experience more critical symptoms, such as severe and persistent diarrhea, as well as sporadic systemic and even fatal diseases. To date, no drugs have been developed to protect against astrovirus infection. Our study provides the first evidence that the integrity of the N-terminal domain of nonstructural protein 1a (nsP1a) is essential for establishing early replication. Central to this process, the di-arginine motifs in the N-terminal domain are

the Department of Pathology studentship from Elisabeth Mann Fund. The funders had no role in study design, data collection and analysis, decision to publish, or preparation of the manuscript. <https://wellcome.org/> <https://www.ukri.org/councils/mrc/> <https://www.newtontrust.cam.ac.uk/>

**Competing interests:** The authors have declared that no competing interests exist.

responsible for ER retention, the formation of functional replication complexes, and viral replication. Therefore, selectively targeting N-terminal domain-mediated ER retention could be a promising therapeutic strategy to effectively control astrovirus infection.

## Introduction

Astroviruses are a family of small non-enveloped (+)ssRNA viruses that infect a wide range of mammalian and avian species. The *Astroviridae* family includes two genera: *Mamastrovirus* and *Avastrovirus*. Humans are susceptible to the classical (HAstV1-8) and genetically divergent non-classical VA/HMO and MLB clades of astroviruses, which cause mild to severe diseases depending on the age and health of an individual [1,2]. Classical astroviruses were discovered in the 1970s and represent one of the leading causes of gastroenteritis in children, the elderly, and those who are immunocompromised. Two groups of non-classical astroviruses were identified much later and are often associated with neurological diseases, such as meningitis and encephalitis [3]. Despite the high zoonotic potential and non-gastrointestinal tropisms [2,4,5], there are still significant gaps in our understanding of the biology of human astroviruses and disease progression. Besides, astrovirus infections are often under-reported despite their high prevalence [6]. Currently, no vaccines or drugs against astroviruses are available. Therefore, it is important to investigate their replication mechanisms to effectively control future outbreaks.

The astrovirus genome is approximately 6.8–7.9 kilobases (kb) in length, linked to genome-linked viral protein (VPg) at the 5' end and polyadenylated at the 3' untranslated region [1,7], with four open reading frames (ORFs): ORF1a, ORF1b, ORFX and ORF2 [8,9]. Both ORF2 and ORFX are translated from subgenomic RNA and encode the structural proteins and viroporin, respectively [8,10]. ORF1b encodes the RNA-dependent RNA polymerase (RdRp), translated following ribosomal frameshifting in the overlapping region between ORF1a and ORF1ab [1,11]. ORF1a encodes a large nonstructural polyprotein (nsP1a), which is processed into several proteins, including the N-terminal protein encoding putative RNA helicase, serine protease, VPg, and p20 protein [1]. The exact number of nonstructural proteins and polyprotein processing rules are yet to be determined.

Replication of (+)ssRNA viruses requires RdRp and other nonstructural proteins that form the viral replication complex. These viruses exploit host membranes to assemble replication complexes (RCs), protect double-stranded RNA (dsRNA) intermediates, and segregate replicating RNAs from translating viral mRNAs [12–14]. In astroviruses, the components of the replication complex contain RdRp, protease, and VPg—three well-characterized enzymatic units [7,11,15]. However, membrane-anchoring and retention strategies are still unknown. The predicted transmembrane (TM) domain located at the N-terminal part of the astrovirus nonstructural protein suggests its involvement in membrane association. Recently, ER-derived membranes were implicated in the formation of double-membrane vesicles during astrovirus infection [16]. However, the exact location, ER membrane specificity, and viral proteins responsible for this remain to be characterized. In addition to the TM domain, the N-terminal domain of the astrovirus polyprotein contains a putative RNA helicase motif [1]. However, its poor conservation and incomplete motif integrity raise questions regarding the functional significance of the proposed helicase.

Here, we demonstrate the function of the N-terminal protein in two astrovirus genotypes, HAstV1 and MLB2. This small membrane protein drives the formation of replication complexes in tight association with perinuclear ER membranes, which is a key feature in a wide

range of astroviruses (HAstV1, HAstV4, MLB1, MLB2, and VA1). We also found that ER retention and the astrovirus replication complex's function depend on the di-arginine motif located in the N-terminal protein. In the future, an improved understanding of astrovirus replication complex formation may represent a promising therapeutic strategy for controlling astrovirus infections in young children, immunocompromised individuals, and farm animals.

## Results

### The putative helicase domain is not conserved and is dispensable for HAstV1 replication

RNA viruses harbor several cis-acting elements that play essential roles in viral RNA replication, translation and assembly of virions [17]. During viral genome replication, these structured RNA elements require RNA helicases or chaperones to facilitate the unwinding and remodeling of double-stranded RNA structures. Helicases use energy derived from NTP hydrolysis to catalyze dsRNA unwinding and contain several conserved motifs, including NTP-binding Walker A and Walker B motifs [18]. Several RNA viruses encode NTPase/RNA helicases, which assist in the unwinding of dsRNA replicative intermediates during virus replication [19]. Interestingly, astrovirus genomes do not have features that can be attributed to a fully functional NTPase/helicase. The only Walker A-like motif can be found in classic human astroviruses, but not in non-classical MLB and VA genotypes (Fig 1A), suggesting poor conservation and questioning the presence of virus-encoded helicases in astroviruses. In addition, this domain is predicted to be attached to the membrane and separated from the rest of the replication module (Fig 1B), which is an unusual localization for RNA-processing enzymes. To address this

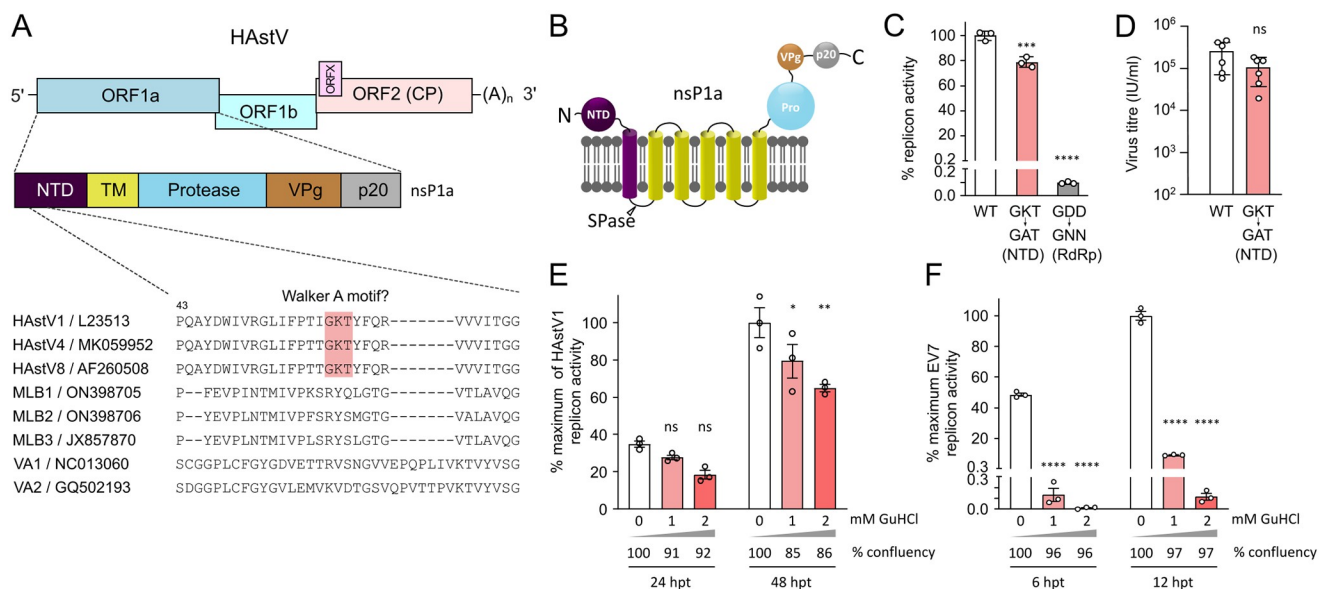


**Fig 1. Analysis of the role of the N-terminal putative helicase in astrovirus replication.** (A) Schematic representation of the astrovirus genome, location of N-terminal domain (NTD), and putative Walker A motif, aligned for several astrovirus genomes. (B) Predicted domain organization of the astrovirus nonstructural polyprotein. SPase, signal peptidase; Pro, protease domain; VPg, viral protein genome-linked. C- and N-terminal ends of polyprotein are indicated. (C) The activity of HAstV1-based Renilla luciferase-expressing replicon was measured in Huh7.5.1 cells at 24 hpt. RdRp knock-out mutant (GDD→GNN) is used as replication-deficient control. (D) The virus titer was measured in Caco2 cells after electroporation of BSR cells with *in vitro* transcribed T7 HAstV1 RNA. (E-F) The effect of guanidine hydrochloride (GuHCl) on the activity of mCherry-expressing astrovirus (E) and enterovirus (F) replicons; hpt, hours post-transfection. The mean cell confluence is provided for each time point. Data are mean ± SEM. \*\*\*\*  $p < 0.0001$ , \*\*\*  $p < 0.001$ , \*\*  $p < 0.01$ , \*  $p < 0.1$ , ns, nonsignificant, using one-way ANOVA (C), Student's t-test (D) or two-way ANOVA (E-F), against wt (C-D) or untreated control (E-F).

<https://doi.org/10.1371/journal.ppat.1011959.g001>

question, the putative Walker A motif in HAstV1 was mutated from GKT to GAT in the context of replicons and infectious viruses. In the replicon system, a minor reduction in activity was observed (Fig 1C), and in the GKT-to-GAT recombinant virus, no significant differences were observed (Fig 1D), whereas mutation of functional GKT/GKS motifs in other viruses is usually lethal [20,21]. This further indicates that the GKT motif is unlikely to play a functionally important role in the HAstV1 replication. In addition, several viral NTPases/helicases, including enterovirus 2C<sup>ATPase</sup> [22], are inhibited by guanidine hydrochloride (GuHCl), resulting in NTPase-specific inhibition of replication [22]. Using HAstV1-based and enterovirus-based replicon systems, we examined the ability of GuHCl to inhibit replication. Unlike previously characterized inhibition in enteroviruses, astrovirus replication was not strongly affected by GuHCl treatment (Fig 1E and 1F). The 20–30% decrease in astrovirus replicon activity is at least partially caused by the decrease in cell confluency in the presence of GuHCl at later time points (Fig 1E), whereas enterovirus replication was efficiently inhibited to ~0.1% (Fig 1F), further confirming that GuHCl-sensitive replicase components are absent in astroviruses. Considering the poor conservation (Fig 1A) and lack of functional effect (Fig 1C–1E) of the putative Walker A motif in HAstV1-based assays, it is plausible to suggest that cellular helicases can be recruited by astrovirus replication complexes (RCs) as an alternative strategy utilized by several virus families [23]. Therefore, the remaining GKT motif may represent an evolutionarily lost NTPase/helicase rather than a functional unit within the astrovirus genome.

### Role, accumulation and localization of NTD in astrovirus replication

To investigate the role(s) of the NTD in virus replication, we engineered HA-tagged astroviruses using classical HAstV1 [8] and neurotropic MLB2 [24] reverse genetics systems by placing an HA-tag sequence in the predicted disordered region between the folded N-terminal part of the protein and the first transmembrane helix. If N-terminal cleavage occurs at the predicted signal peptidase (SPase) cleavage site, the molecular weight of the N-terminal HA-tagged astrovirus protein is predicted to be 21–22 kDa (Fig 2A). MLB2-HA virus was successfully rescued, and growth kinetics was assessed in Huh7.5.1 cells, displaying a minor delay in growth (Fig 2B), which is common for tagged viruses with small genomes. The rescue of HAstV1-HA was successful following the transfection in BSR cells but not on passaging in Caco2 cells (Fig 2C). This could indicate a defect specific to infection in Caco2 cells and potential differences in antiviral responses between different cell lines. The accumulation of ~14 kDa HA-tagged product was detected in HA-tagged but not in wt astrovirus-infected cells (Fig 2D and 2E). Due to the differences in predicted and observed sizes of HA-tagged proteins, we analyzed the same samples in Bis-Tris acrylamide gels, where ~20 kDa HA-tagged products were detected, confirming their aberrant mobility in Tris-glycine acrylamide gel systems (Fig 2F) [25]. Capsid accumulation showed a slight delay in HA-tagged MLB2 samples when compared to the wt virus, consistent with the delay in virus growth (Fig 2D). Next, we analyzed the same viral products using immunofluorescence of the virus-infected cells at 24 hpi. Interestingly, we observed a distinct perinuclear localization of HA-tagged protein for both viruses. In contrast, the capsid protein was dispersed throughout the cytoplasm (Fig 2G and 2H), most likely due to its excess and less likely membrane association. Notably, the cytoplasmic distribution of the capsid was more evident in Huh7.5.1 cells due to their larger cytoplasmic space (Fig 2G).

### Astrovirus replication complexes are associated with endoplasmic reticulum membranes, close to the nuclear periphery

Similar to other (+)ssRNA viruses, the replication of human astroviruses is associated with the host endoplasmic reticulum (ER) by forming double-membrane vesicles [16]. However, the

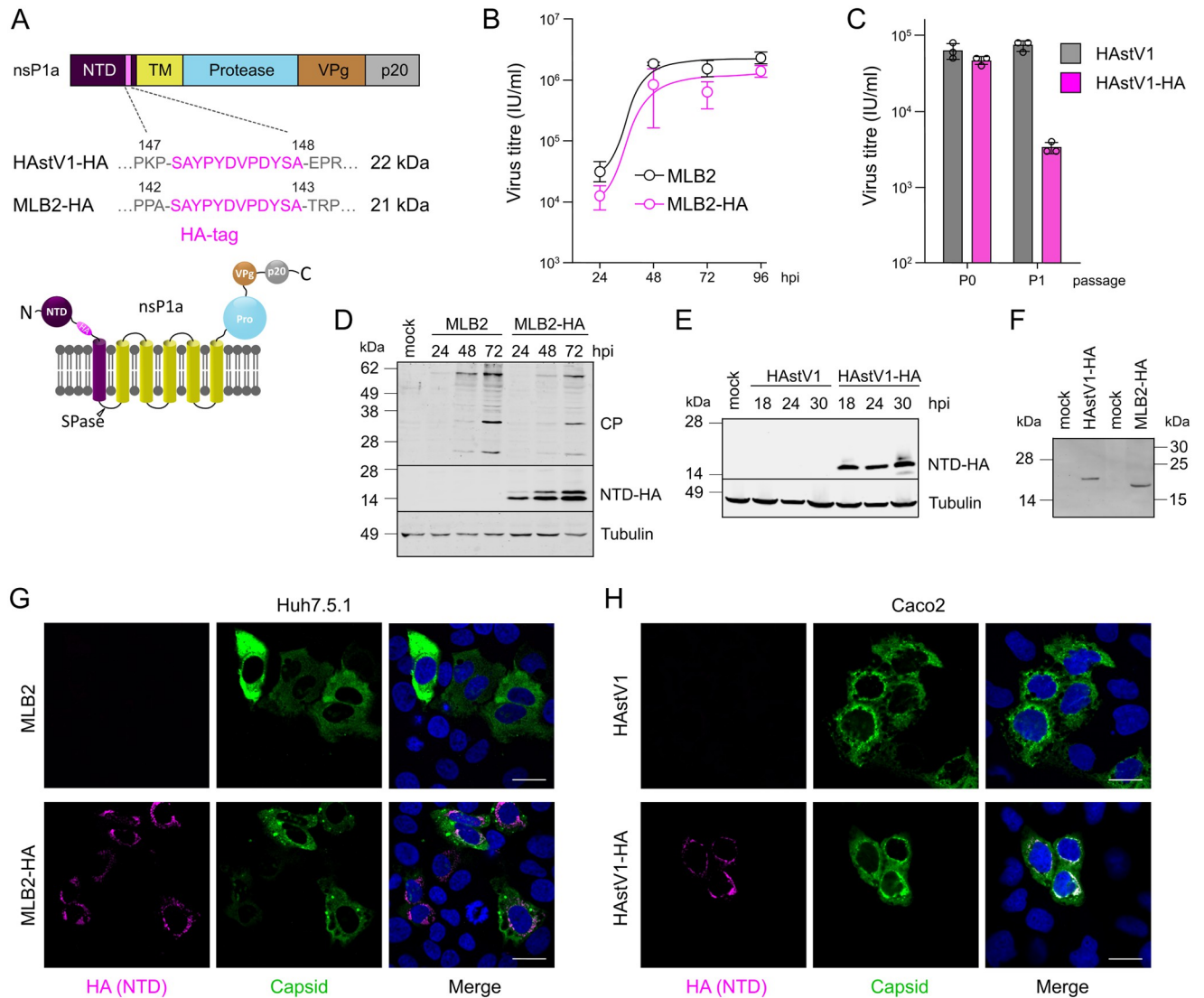


**Fig 2. Design and characterization of HA-tagged astroviruses.** (A) Schematic representation of astrovirus ORF1a polyprotein with HA-tagged NTD domain. The amino acid positions are indicated for each astrovirus strain (top panel). Predicted membrane topology for HA-tag within nsP1a polyprotein (bottom panel). Predicted molecular weight is provided for HAstV1-HA and MLB2-HA SPase-cleaved N-terminal protein. (B) Multistep growth curves of MLB2 and MLB2-HA viruses in Huh7.5.1 cells. Cells were infected at MOI 0.1 (passage 2), and virus titer was measured from the extracellular fractions in triplicates. Data are mean ± SEM. (C) Titers of rescued (passage 0) and passaged (passage 1 in Caco2 cells) HAstV1 and HAstV1-HA viruses. (D) Huh7.5.1 cells were infected at MOI 0.1 (passage 2), harvested at indicated hpi and analyzed by western blotting with anti-CP and anti-HA antibodies. (E) Caco2 cells were infected at MOI 1 (passage 0), harvested at indicated hpi and analyzed by western blotting with anti-HA antibodies. (F) The 24 hpi samples from (D) and (E) were analyzed using Bis-Tris acrylamide gel electrophoresis. (G-H) Representative confocal images of fixed and permeabilized infected cells visualized for MLB2 (G) or HAstV1 (H) CP (green) and HA-tag (magenta). Nuclei were stained with Hoechst (blue). Scale bars are 25 μm (G-H).

<https://doi.org/10.1371/journal.ppat.1011959.g002>

mode of RC formation and its retention within the ER membranes still needs to be determined. To systematically investigate the cellular localization of astrovirus replication sites, we used five available astrovirus strains (HAstV1, HAstV4, MLB1, MLB2 and VA1) and infected two different cell lines (Huh7.5.1 and Caco2) that support selected astrovirus replication and spread. Staining with anti-dsRNA antibody, a hallmark of (+)ssRNA replication sites, revealed perinuclear localization of RCs in Caco2 (Fig 3A) and Huh7.5.1 (Fig 3B) cells. The dsRNA-specific signal overlapped with ER-specific staining only very close to the nuclear periphery, but

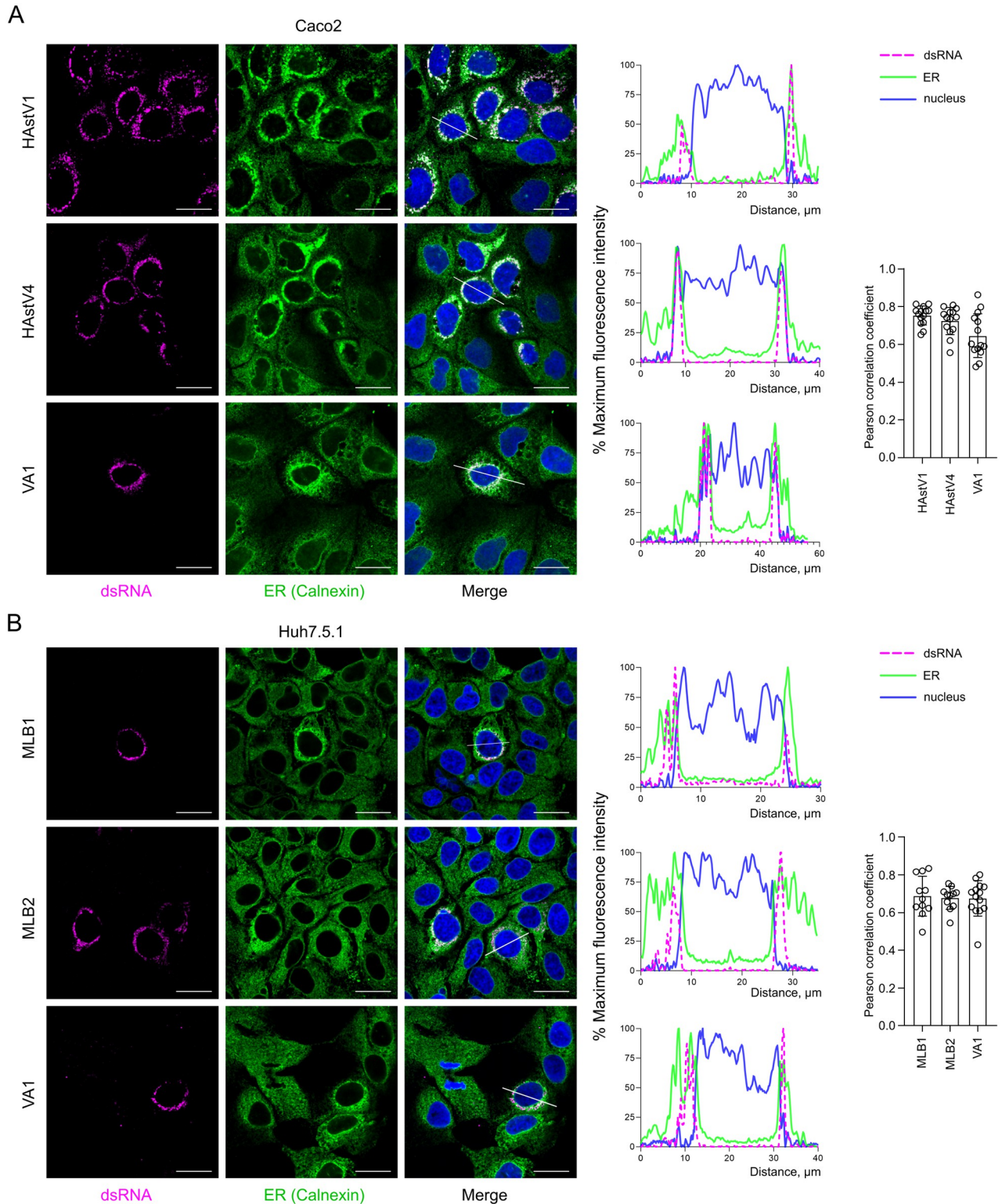


**Fig 3. Astrovirus replication sites are associated with the perinuclear ER membranes.** (A) Caco2 cells were infected with HAstV1, HAstV4 and VA1 astroviruses. (B) Huh7.5.1 cells were infected with MLB1, MLB2 and VA1 astroviruses. (A-B) Representative confocal images of fixed and permeabilized cells visualized for dsRNA (magenta) and ER (calnexin, green). Nuclei were stained with Hoechst (blue). Scale bars are 25 μm. Intensity profiles of dsRNA (magenta), calnexin (green) and nuclear staining (blue) were obtained using ImageJ software, along a straight line shown on the merged image crossing the representative cell. Quantification of co-localization of dsRNA with calnexin. The Pearson correlation coefficient was calculated for 12 images in each experiment.

<https://doi.org/10.1371/journal.ppat.1011959.g003>

not further in the cytoplasm in all tested astrovirus-infected cells (Fig 3). Co-staining with lamin, a component of the nuclear membrane, revealed weak co-localization (Fig 4), confirming the preferential perinuclear localization of the astrovirus RCs. This was further confirmed by quantification using Pearson correlation coefficient (PCC) indicating a correlation of ER-dsRNA (mean PCC > 0.6) but not lamin-dsRNA (mean PCC < 0.4) signals (Figs 3 and 4). These results suggest the specific targeting of RCs to the perinuclear ER membranes and the possible involvement of NTD in this process (Fig 2G and 2H).

### During astrovirus infection, the NTD is colocalized with replicating RNA and perinuclear ER membranes

To investigate the localization of NTD during astrovirus infection, Caco2 and Huh7.5.1 cells were infected with HAstV1-HA and MLB2-HA, respectively. As expected, a strong overlap between dsRNA- and NTD-specific signals was observed (mean PCC > 0.7, Fig 5), confirming the previous observations. Consistent with the staining obtained with wt astrovirus strains (Figs 3 and 4), HA-tagged NTD-specific localization followed the same overlapping perinuclear ER- (mean PCC > 0.6) and weak lamin-specific (mean PCC < 0.5) pattern (Fig 5).

### The NTD is colocalized with protease and RdRp during astrovirus infection

First, we developed a set of antibodies for specific immune detection of the following astrovirus proteins: VA1 capsid protein (CP), HAstV1 protease and RdRp, and MLB2 protease. The folded region of the indicated proteins possessing a C-terminal 8×His-tag was used for bacterial expression and affinity purification, resulting in homogeneous proteins of the expected sizes (Fig 6A). Each purified recombinant protein was used for the production and affinity-based purification of antibodies [24]. VA1 CP-specific antibody was used to titrate VA1 stocks and identify VA1-infected cells by immunofluorescence (Figs 3, 4 and 6B), whereas antibodies against nonstructural proteins were used to visualize replication complex-specific components (Fig 6B and 6C).

To identify the components of RCs, we performed several pairwise immunofluorescent stainings, where a combination of antibodies would allow such an approach (e.g. combination of mouse and rabbit-derived antibodies). The pattern of VA1 and MLB2 capsid proteins was distinct from dsRNA-specific staining (PCC < 0.6, Fig 6B), following the same trend as NTD-CP co-staining (Fig 2G and 2H).

Out of several nonstructural proteins, RdRp and protease are usually found within RCs of (+)ssRNA viruses [26], performing RNA synthesis and cleavage of the nonstructural polyprotein, respectively. Due to the availability of antibody combinations, we could test several possibly co-localized pairs of proteins. The strong co-localization is observed between all three replication components: dsRNA, protease and RdRp (PCC > 0.8, Fig 6C), recapitulating the NTD-dsRNA pattern (Fig 5).

To further investigate co-localization of dsRNA, protease, RdRp and NTD, we adapted a proximity ligation assay (PLA) that permits the detection of protein-protein or protein-RNA interactions in situ (at distances < 40 nm). In agreement with previous observations (Fig 6C), we detected positive PLA signals for RdRp-dsRNA (in HAstV1 and HAstV1-HA infected cells) and protease-dsRNA (in HAstV1, HAstV1-HA, MLB2 and MLB2-HA infected cells), indicating proximity of dsRNA, RdRp and protease. In concordance with immunostaining of HA-tagged viruses (Fig 5), the specific NTD-protease/NTD-RdRp PLA signal was detected in HAstV1-HA-infected Caco2 cells, and NTD-protease PLA foci were observed both in HAstV1-HA and in MLB2-HA-infected cells (Fig 6D and 6E).

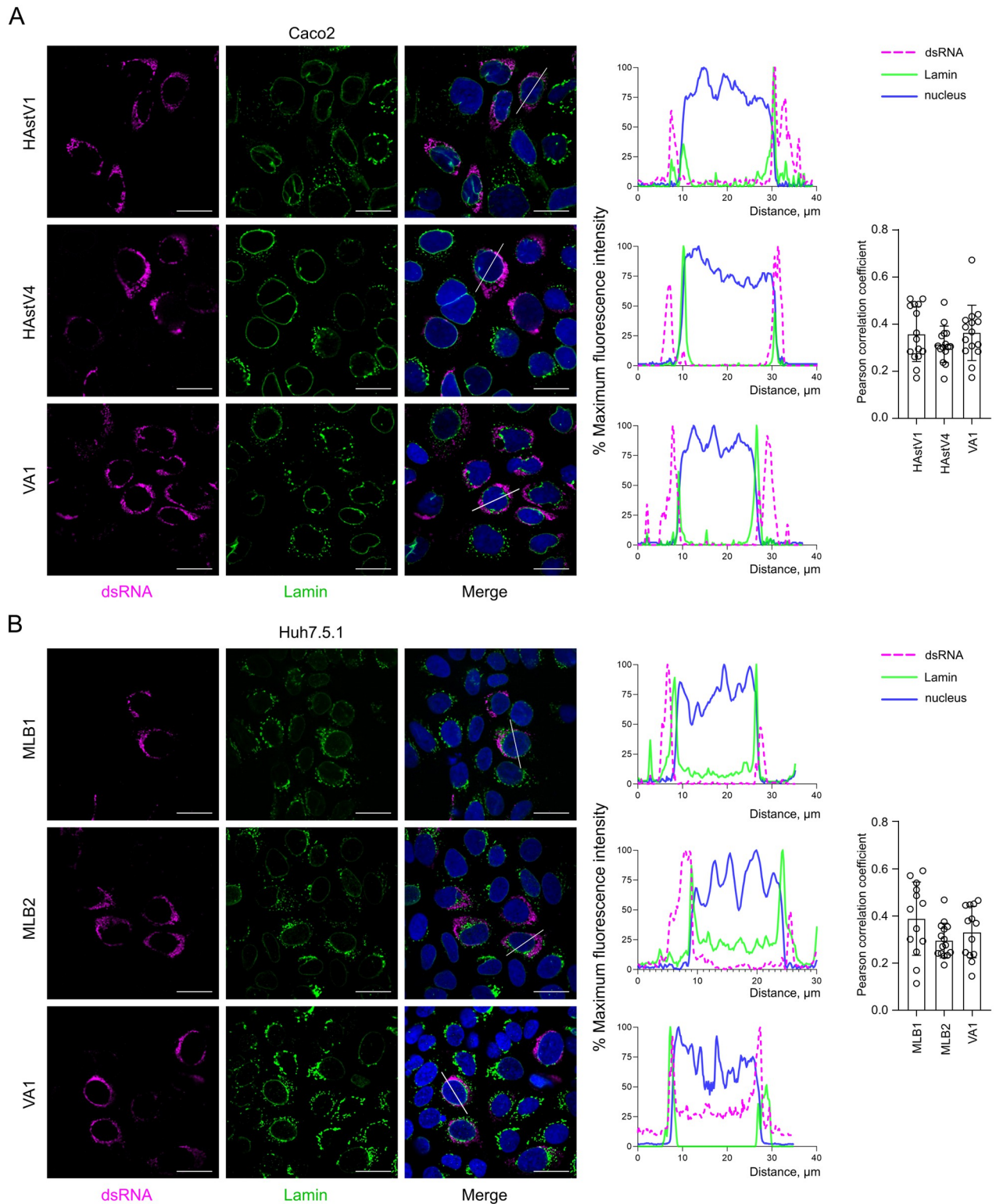


**Fig 4. Astrovirus replication sites demonstrate perinuclear ER localization.** (A) Caco2 cells were infected with HAstV1, HAstV4 and VA1 astroviruses. (B) Huh7.5.1 cells were infected with MLB1, MLB2 and VA1 astroviruses. (A-B) Representative confocal images of fixed and permeabilized cells visualized for dsRNA (magenta) and nuclear lamin (green). Nuclei were stained with Hoechst (blue). Scale bars are 25  $\mu\text{m}$ . Intensity profiles of dsRNA (magenta), lamin (green) and nuclear staining (blue) were obtained using ImageJ software, along a straight line shown on the merged image crossing the representative cell. Quantification of co-localization of dsRNA with lamin. The Pearson correlation coefficient was calculated for 12 images in each experiment.

<https://doi.org/10.1371/journal.ppat.1011959.g004>



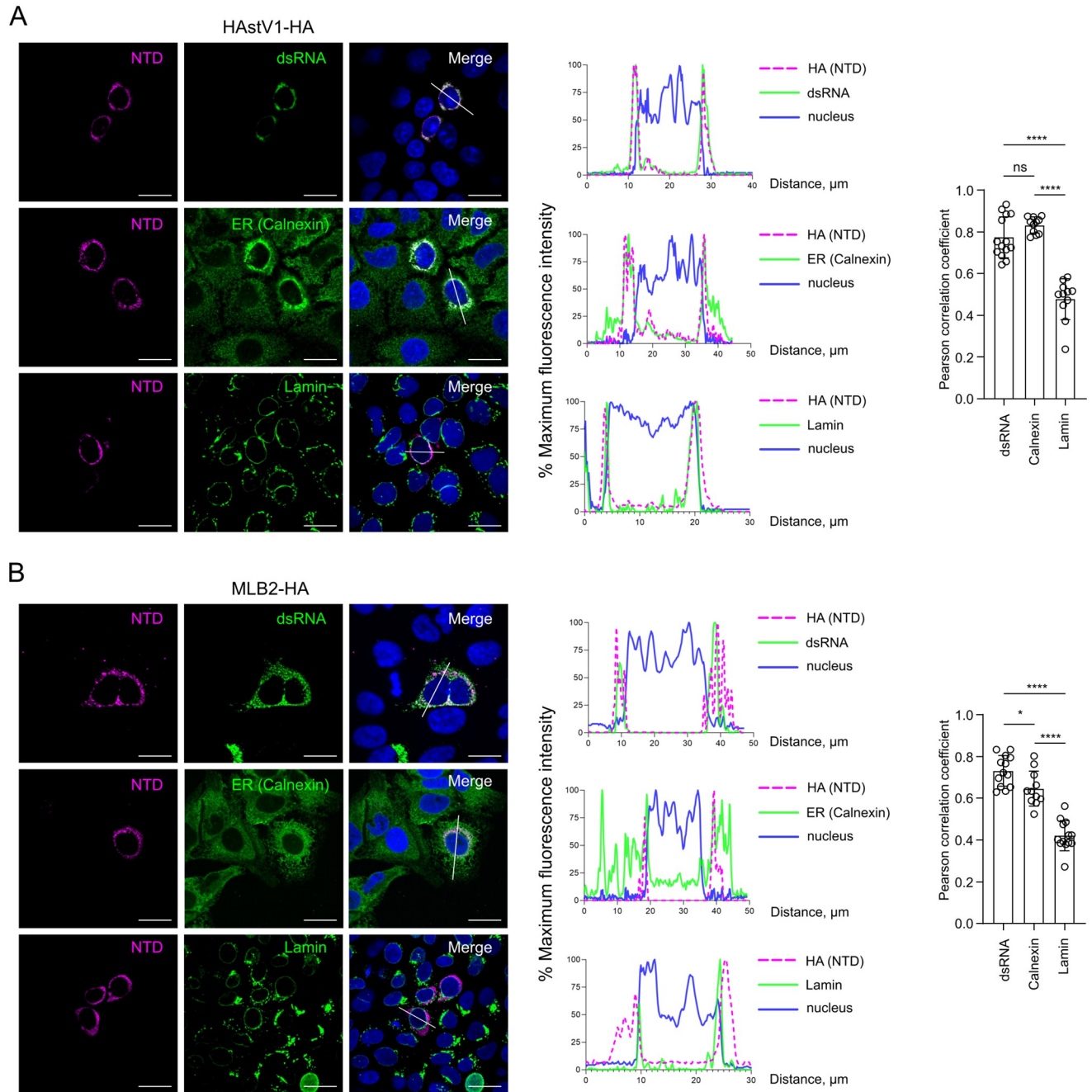


**Fig 5. Astrovirus NTD is associated with RNA replication sites.** (A) Caco2 cells were infected with HAstV1-HA. (B) Huh7.5.1 cells were infected with MLB2-HA. (A-B) Representative confocal images of fixed and permeabilized cells visualized for HA-tag (NTD, magenta), dsRNA (green), ER (calnexin, green), and lamin (green). Nuclei were stained with Hoechst (blue). Scale bars are 25  $\mu\text{m}$ . Intensity profiles of NTD (magenta), dsRNA (green), ER (green), lamin (green), and nuclear staining (blue) were obtained using ImageJ software, along a straight line shown on the merged image crossing the representative cell. Quantification of co-localization of NTD with dsRNA, calnexin, and lamin. The Pearson correlation coefficient was calculated for 12 images in each experiment. Data are mean  $\pm$  SEM. \*\*\*\*  $p < 0.0001$ , \*  $p < 0.05$ , ns, nonsignificant, using one-way ANOVA test against wt.

<https://doi.org/10.1371/journal.ppat.1011959.g005>

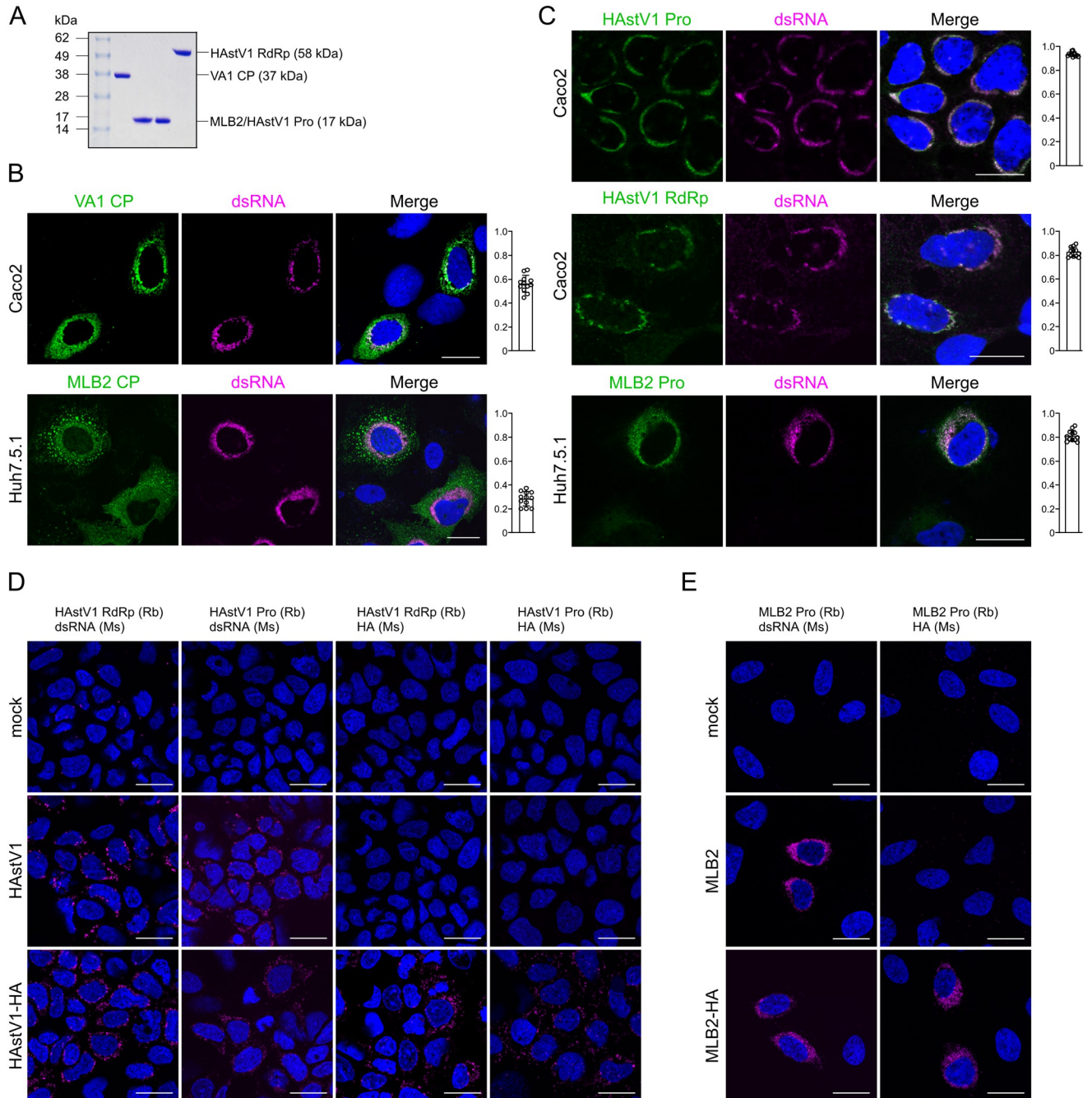


**Fig 6. Astrovirus replication sites are tightly associated with dsRNA, NTD, protease and RdRp, the capsid protein is dispersed throughout the cytoplasm.** (A) Coomassie-stained SDS-PAGE profile of purified proteins from *E. coli* (left-to-right): folded domains of VA1 capsid protein (CP), MLB2 and HAstV1 protease and HAstV1 RdRp. Predicted molecular weight is given for each purified protein domain. (B) The indicated cell line was infected with MLB2 (top) or VA1 (bottom) and stained for dsRNA (magenta) and virus-specific capsid protein (green). Nuclei were stained with Hoechst (blue). (C) The indicated cell line was infected with HAstV1 or MLB2 and stained for dsRNA (magenta) and virus-specific nonstructural proteins (green). Nuclei were stained with Hoechst (blue). The quantification of co-localization of dsRNA with indicated virus protein is shown on the right (B-C). The Pearson correlation coefficient was calculated for 12 images in each experiment (B-C). (D-E) Proximity ligation assay (PLA) for key RC components in astrovirus-infected cells. Caco2 (D) and Huh7.5.1 (E) cells were infected with the viruses indicated on the left of each panel, followed by PLA staining using pairs of rabbit (Rb) and mouse (Ms) derived antibodies indicated on top of each panel. A representative experiment of two independent repeats is shown. Scale bars are 25  $\mu$ m (B-E).

<https://doi.org/10.1371/journal.ppat.1011959.g006>

Taken together, we confirm the association of the key components of RNA RCs: dsRNA, protease, RdRp, and NTD (Figs 5 and 6B–6E).

Overall, these results confirmed the proximity of the astrovirus NTD with RCs, raising an important question: what drives the NTD to the perinuclear ER membranes and how does this affect astrovirus replication?

### Di-arginine motifs in NTD are responsible for perinuclear ER localization and astrovirus replication

ER targeting of RCs in (+)ssRNA viruses can be achieved through various mechanisms [27]. In astroviruses, the NTD, followed by transmembrane helices, represents a unique combination to target the nonstructural polyprotein to the correct position within the infected cell. We explored the power of molecular mimicry used by many viruses to identify the potential residues responsible for ER targeting that were predicted using the ELM web server (<http://elm.eu.org/>) [28,29]. The search revealed the presence of conserved di-arginine motifs (Fig 7A),

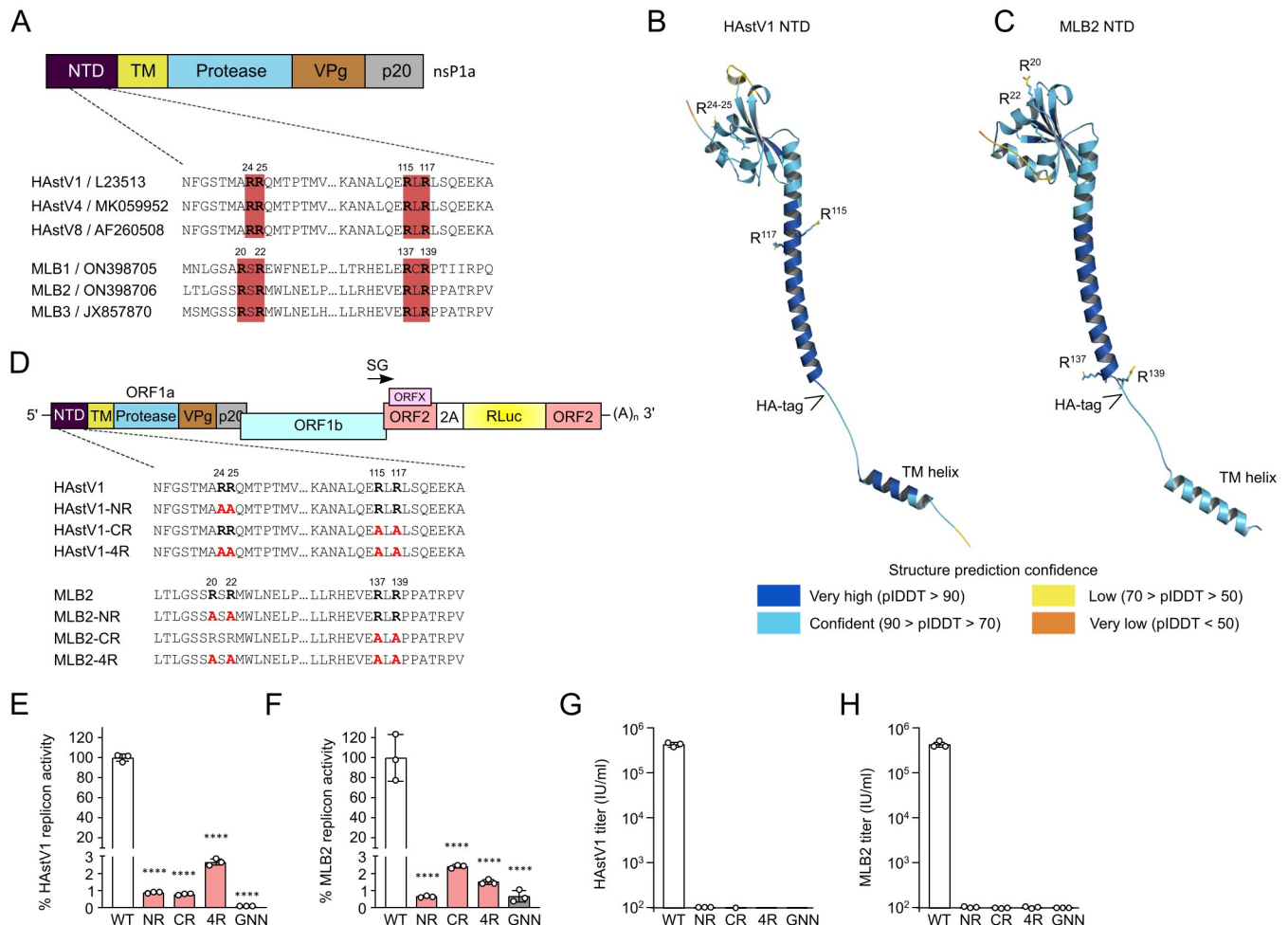


**Fig 7. Di-arginine motifs in NTD are required for virus replication.** (A) Schematic representation of astrovirus nsP1a polyprotein with di-arginine motifs. The amino acid positions are indicated for each astrovirus strain. (B–C) 3D model for wt HAstV1 (B) and wt MLB2 (C) NTD predicted with AlphaFold 3. The positions of the di-arginine motifs, the inserted HA-tag (insertion position only), and the transmembrane (TM) helix are indicated. (D) Schematic representation of astrovirus replicon with introduced R-to-A mutations. The mutant annotation is shown on the left. (E–F) Relative luciferase activities of HAstV1 (E) and MLB2 (F) based replicons in Huh7.5.1 cells at 24 hours post-transfection. Data are mean ± SD. \*\*\*\*  $p < 0.0001$ , using one-way ANOVA test against wt. RdRp knock-out mutant (GDD→GNN) is used as replication-deficient control. (G–H) Titers (infectious units per ml) of recombinant viruses after RNA electroporation of BSR (HAstV1) or Huh7.5.1 (MLB2) cells followed by titration on Caco2 (HAstV1, G) or Huh7.5.1 (MLB2, H) cells.

<https://doi.org/10.1371/journal.ppat.1011959.g007>

which were defined by two consecutive arginine residues (RR) or with a single residue insertion (RXR). This motif is characteristic of several membrane proteins with ER localization and allows for correct folding and membrane association. The functional motif needs to be exposed to the cytoplasm and requires distinct proximity to the TM region, thus fulfilling the criteria for a predicted astrovirus nonstructural polyprotein (Figs 1B and 7A) [30].

The structure of astrovirus NTD is unknown, so we performed a structure prediction using the AlphaFold 3 server [31–33] and mapped identified di-arginine residues and the position of the HA-tag in HAstV1 and MLB2 NTD (Fig 7B and 7C). Both di-arginine motifs were mapped to the surface-exposed cytoplasmic domain of the NTD, suggesting that these residues could have a functional impact on the properties of NTD. The transmembrane helix was predicted at the end of NTD and should not be affected by mutations or the inserted HA-tag (Fig 7B and 7C).

To investigate the function of the di-arginine motifs of NTD in the virus life cycle, arginine-to-alanine mutations were introduced into replicons and full-length infectious clones of HAstV1 and MLB2 astroviruses (Fig 7D). Replication was drastically decreased in all mutant replicons (>95%, Fig 7E and 7F) and all di-arginine mutant viruses were not viable (Fig 7G and 7H), confirming the critical role of both di-arginine motifs in the virus life cycle.

To link the replication defect to the specific ER localization performed by the NTD, the same subset of mutations (Fig 7A) was introduced into a mammalian expression vector that encodes only 187 (MLB2) or 190 (HAstV1) amino acid residues of the HA-tagged NTD (Fig 8A). All NTD variants containing mutated N-terminal di-arginine motifs showed reduced amounts of protein (Fig 8B and 8C), suggesting that the stability of the protein can be dictated by the correct ER targeting mediated by the N-terminal di-arginine (NR) motif. Poor expression of NR and 4R mutants could be explained by protein degradation due to mislocalization and/or misfolding of the protein and thus precluded their usage in the following immunofluorescent-based studies.

The perinuclear localization of overexpressed wt NTD-HA (Fig 8D and 8E, top panels) recapitulated the NTD-HA localization in virus-infected cells (Fig 5), suggesting the role of this domain in the correct anchoring of astrovirus RCs. Perinuclear ER staining was drastically altered in C-terminal arginine-to-alanine (CR) mutants, resulting in a diffuse ER pattern in cells expressing both HAstV1 and MLB2 NTD-HA protein, despite the TM helix and N-terminal di-arginine motif remaining unmodified. The changes in the overlap signal between NTD-HA and ER were also analyzed using Manders's coefficient ( $M_2$ ), which further confirmed the redistribution of NTD-HA signal in the population of analyzed cells (Fig 8D and 8E).

Taken together, these results (Figs 7 and 8) provide evidence for the distinct features of N- and C-terminal di-arginine motifs and the functional role of the NTD in the membrane association of astrovirus RC, a prerequisite for efficient replication. The functional significance of other viral/host proteins in this process remains to be characterized.

## Discussion

In this study, we investigated the role of the astrovirus N-terminal protein in ER membrane tethering and the formation of functional RCs. We demonstrate that the putative helicase is unlikely to be a functional unit within astrovirus RCs. Instead, the di-arginine signature-driven ER membrane localization and replication represents a key role of the N-terminal protein in the astrovirus replication cycle.

Numerous positive-sense RNA viruses encode RNA helicases, while others depend on cellular counterparts in their absence [19,23]. Interestingly, astrovirus genomes encode a single

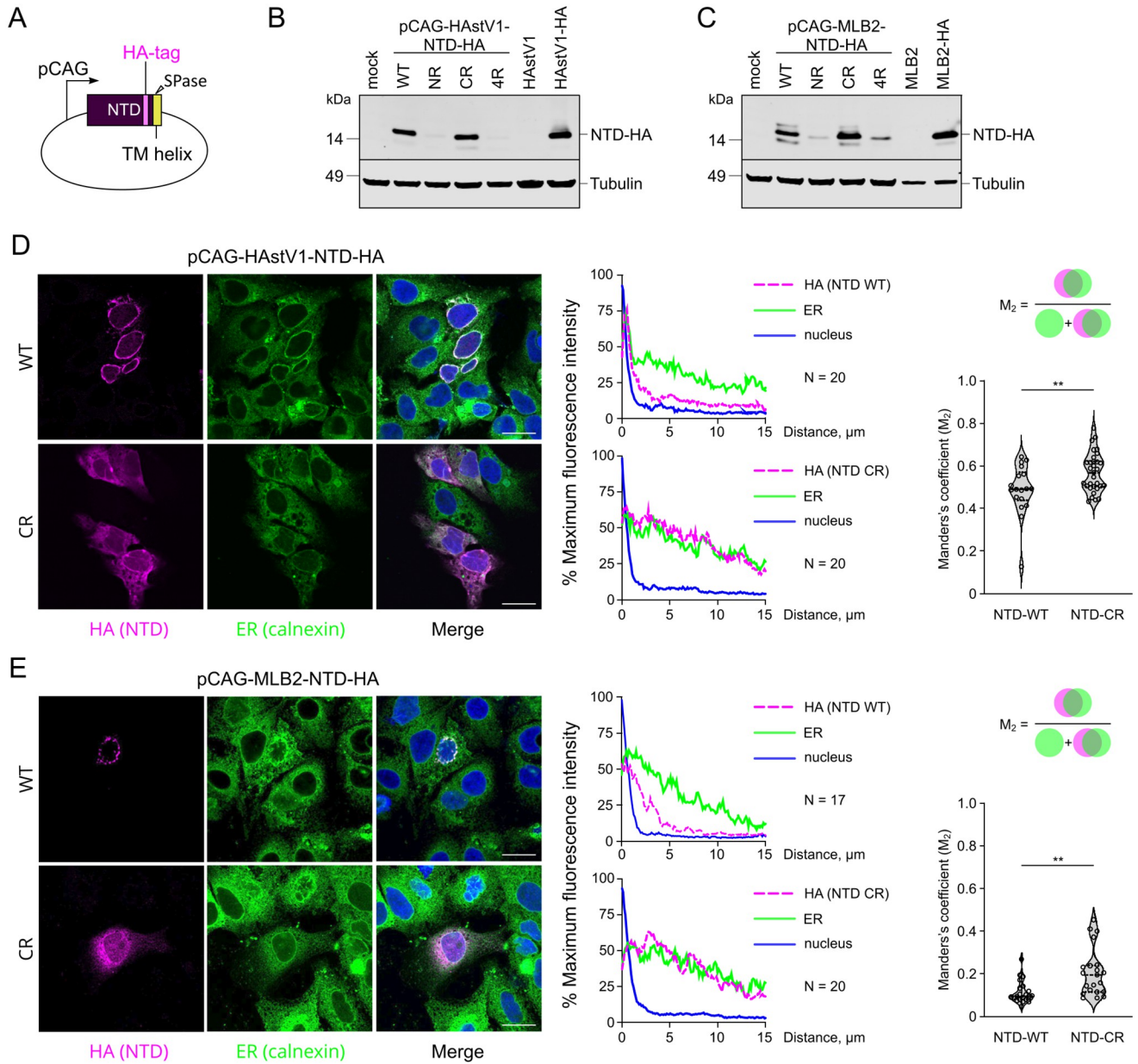


**Fig 8. Di-arginine motifs define the efficient expression and perinuclear ER localization of NTD.** (A) Schematic representation of CAG promoter containing mammalian expression vector used to over-express HA-tagged NTD in Huh7.5.1 cells. (B-C) Huh7.5.1 cells were electroporated with pCAG plasmids expressing wt and mutant NTD-HA and analyzed by western blotting with anti-HA and anti-tubulin antibodies. Lysates obtained from infected cells were used as a control. (D-E) Huh7.5.1 cells were electroporated with pCAG plasmids expressing wt and mutant NTD-HA and analyzed by immunofluorescence. Representative confocal images of fixed and permeabilized cells visualized for HA-tag (NTD, magenta) and ER (calnexin, green). Nuclei were stained with Hoechst (blue). Scale bars are 25  $\mu$ m. Averaged intensity profiles of NTD (magenta), ER (green) and nuclear staining (blue) were obtained using ImageJ software, along a straight line spanning from the nucleus to the plasma membrane of 17–20 transfected cells. The changes in the overlap signal between NTD-HA and ER were compared using Manders coefficient ( $M_2$ ).

<https://doi.org/10.1371/journal.ppat.1011959.g008>

Walker A-like motif that can be found in classic human astroviruses but not in the newly emerging human (Fig 1A) and avian astroviruses [34]. Consistent with poor conservation, mutation of the GKT motif was not detrimental to HAstV1 replication and life cycle (Fig 1). The absence of evidence of a functional helicase in the genome of astroviruses suggests

dependence on host proteins with NTPase/helicase activity. Notably, proteomic analysis of HAstV8-infected Caco2 cells showed enrichment of membrane-only fractions with the cellular RNA helicase DDX23, detected alongside viral RdRp and protease, established components of RCs [35]. Additionally, siRNA-mediated depletion of DDX23 significantly decreased virus replication [35], indicating the host helicase dependence of astrovirus replication. In a recent transcriptomic analysis of HAstV1-infected Caco2 cells, cellular helicases HELZ2 and DDX58 transcripts were found to be upregulated in infected cells [16], providing more candidates for the host helicases that can be involved in the RNA replication process.

The correct formation of (+)ssRNA virus RCs is mediated by the recruitment of cellular membranes that prevent immune detection of viral RNA, separate the processes of replication and translation, and increase the local concentration of active replication components, both viral and cellular [12–14]. Viruses employ a range of strategies to ensure the correct association of replication-competent virus-host replication machinery. Co-opting the ER for this purpose has been described for numerous RNA viruses including the *Flaviviridae*, *Coronaviridae*, *Picornaviridae* [36] families, and has also been suggested for astroviruses [16,35,37]. We confirm this localization and identify perinuclear ER membranes as the preferential RNA replication site (Fig 3), similar to several other RNA viruses [38–40]. Besides ER, many RNA viruses have evolved to recruit alternative subcellular membranes, such as mitochondrial, Golgi, endosomal, and lysosomal membranes [41,42].

The proposed involvement of the N-terminal part of the nonstructural polyprotein in the positioning of the whole replication complex is a convenient strategy to ensure translocation across the ER membrane which can be mediated by the N-terminal signal/sorting peptide [43]. In astroviruses, the N-terminal protein, followed by transmembrane helices, is ideally positioned to target the nonstructural polyprotein to cellular membranes. Of the multiple strategies of ER membrane integration [30,43], we found that astroviruses most likely use di-arginine-based ER-sorting motifs [44] to anchor and assemble RCs. This strategy is used by several mammalian (lip35, GABA<sub>B</sub>, Kir6.2) [30], plant (AtGCSI) [45], and viral (hepatitis B virus S) [46] proteins for membrane trafficking [30]. We demonstrated that two predicted pairs of N-terminal di-arginine motifs are essential for virus replication and are responsible for the perinuclear ER localization of the N-terminal protein (Figs 6–8). This links two crucial functions together: the correct localization of the RC components and their activity (Fig 9). As many viruses exploit the ER during infection, pharmacological strategies aimed at disrupting virus-ER traffic/interactions or ER morphogenesis should, in principle, lead to the generation of broad-spectrum antiviral targets.

Perinuclear localization of replication complexes has been reported for several RNA viruses. In particular, perinuclear ER-specific replication is a hallmark of the replication of brome mosaic virus [38,47], flaviviruses [39,48], and several other virus families. The mechanisms of perinuclear ER targeting represent a diverse set of approaches based on molecular mimicry of ER-residing proteins and recruitment of related ER-associated proteins [49]. We demonstrate a similar strategy employed by astroviruses thus expanding the list of viral ER hijackers. An outstanding question is how host factors cooperate with virus-encoded di-arginine motifs to construct the ER-derived replication organelle and how virus assembly and maturation are linked to the modified cellular membranes.

Altogether, our findings provide insight into astrovirus replication and the involvement of the N-terminal nonstructural protein in the correct positioning of RCs. Future studies will address the exact host components involved in the formation of active replication organelles and describe the topology and functionality of viral nonstructural proteins. Understanding virus replication mechanisms will potentially lead to the development of future therapeutics.

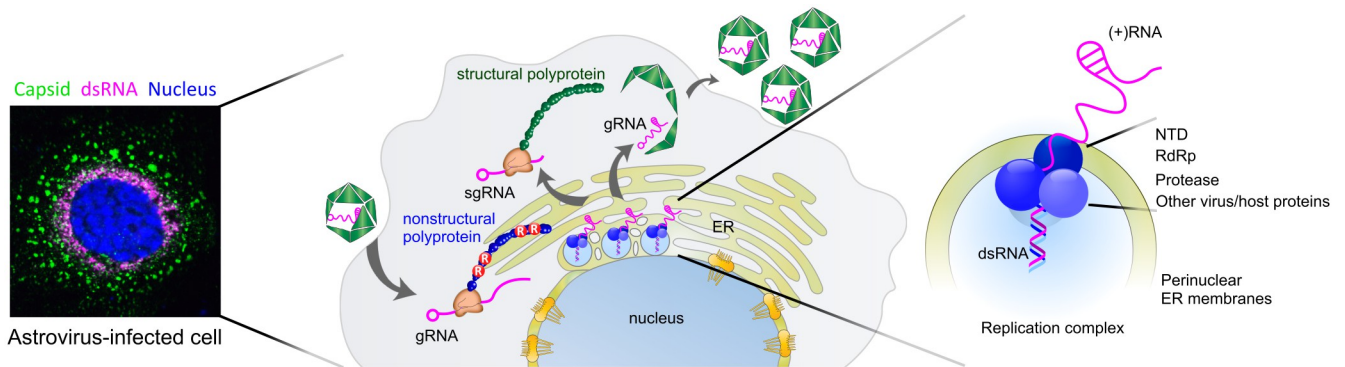


**Fig 9. The proposed mechanism of NTD-directed formation of astrovirus replication complex.** The translation of astrovirus nonstructural polyprotein begins with the NTD, that is anchored to ER membranes through cooperative interactions of charged arginine residues. Non-structural proteins including viral RdRp, protease, and NTD, form the replication complex in tight association with perinuclear ER membranes and other virus/host proteins. Newly synthesized viral genomic and subgenomic RNAs (gRNA and sgRNA) are used for translation, replication, and/or packaging.

<https://doi.org/10.1371/journal.ppat.1011959.g009>

## Materials and methods

### Cells

BSR cells (single clone of BHK-21 cells) were maintained at 37°C in DMEM supplemented with 5% fetal bovine serum (FBS), 1 mM L-glutamine and antibiotics. Caco2 and Huh7.5.1 cells (Apath, Brooklyn, NY) were maintained in the same media supplemented with 10% FBS and non-essential amino acids. All cells were tested mycoplasma negative throughout the work (MycoAlert Mycoplasma Detection Kit, Lonza).

### Virus strains and virus-specific antibodies

HAsV1 (pAVIC1, L23513.1), MLB1 (pMLB1, ON398705) and MLB2 (pMLB2, ON398706) were derived from reverse genetics clones. VA1 astrovirus was kindly provided by David Wang (University of St Louis, USA) and clinical HAsV4 was kindly provided by Susana Guix (University of Barcelona, Spain). HAsV1 CP was detected using Astrovirus 8E7 antibody (Santa Cruz Biotechnology, sc-53559, 1:750). MLB1 and MLB2 CP were detected using the previously described custom antibody [24].

### Plasmids and cloning

Reverse genetics and replicons of the human astroviruses MLB2 [24] and HAsV1 [8,50] were previously described. HA-tagged human astroviruses (MLB1 and HAsV1) were generated by site-directed mutagenesis. The coding sequence of the HA-tag was inserted in the nsP1a as shown in Fig 2A. The resulting infectious clones were designated as HAsV1-HA and MLB2-HA.

For mammalian expression of the MLB2 and HAsV1 nsP1a N-terminal domain, the coding sequence of the HA-tagged N-terminal domain from corresponding HA-tagged virus was inserted into vector pCAG-PM [8] using AflIII and PacI restriction sites. The resulting constructs—designated pCAG-HAsV1-NTD-HA and pCAG-MLB2-NTD-HA—were confirmed by sequencing. All mutations were introduced using site-directed mutagenesis and confirmed by sequencing.

EV7 replicon was generated by insertion of mCherry coding sequence flanked by 3Cpro and 2A cleavage sites between nucleotides 794 and 3323 of pT7-EV7 plasmid (AF465516) [51].

For bacterial expression of folded domains of VA1 CP (68–392 aa in ORF2, NC\_013060.1), HAstV1 Pro (432–587 aa in ORF1a, L23513.1), HAstV1 RdRp (17–519 aa in ORF1b, L23513.1) and MLB2 Pro (391–546 aa in ORF1a, ON398706), the indicated coding sequence was PCR amplified and inserted into the T7 promoter-based pExp-MBP-TEV-Chis (CP) or pExp-His-MBP-TEV (Pro, RdRp) expression plasmid containing N-terminal MBP fusion tag, TEV protease cleavage site and N- or C-terminal 8×His-tag.

### Purification of His-tagged astrovirus proteins and generation of specific antibodies

The VA1 CP, HAstV1 Pro, HAstV1 RdRp and MLB2 Pro proteins were produced in Rosetta 2 (DE3) cells (Novagen) cultured in 2×YT media with overnight expression at 18°C induced with 0.4 mM IPTG. The proteins were purified first by immobilized metal affinity chromatography using PureCube Ni-NTA resin and then by affinity chromatography using amylose resin (NEB). MBP fusion tag was removed by the cleavage with TEV protease (produced in-house). Proteins were further purified by heparin chromatography using HiTrap Heparin HP or anion-exchange chromatography using HiTrap Q-HP 5 ml column (Cytiva) and, finally, by size exclusion chromatography using a Superdex 200 16/600 column (Cytiva). Protein solution in 50 mM Na-phosphate pH 7.4, 300 mM NaCl, 5% glycerol was concentrated to 2 mg/ml and used for immunization.

Antibodies against indicated proteins were generated in rabbits using 5-dose 88-day immunization protocol. Sera were used for specific affinity purification, followed by purification of specific IgG fractions (BioServUK Ltd).

### Recovery of recombinant viruses from T7 *in vitro* transcribed RNAs

The linearised infectious clones of HAstV1 (pAVIC1, L23513.1) and MLB2 (pMLB2, ON398706) were used to produce capped T7 RNA transcripts using T7 mMESSAGE mMACHINE Transcription kit (ThermoFischer, AM1344) according to the manufacturer's instructions. Recombinant viruses were recovered from T7 transcribed RNA using electroporation of Huh7.5.1 cells (MLB2) or BSR cells (HAstV1) in PBS at 800 V and 25 μF using a Bio-Rad Gene Pulser Xcell electroporation system. For HAstV1 passaging, the collected supernatant was treated with 10 μg mL<sup>-1</sup> trypsin (Type IX, Sigma, #T0303) for 30 min at 37°C, diluted 5 times with serum-free media, and used for infection of Caco2 cells. The passaging of MLB2 was performed on Huh7.5.1 cells without trypsin. Recombinant (HAstV1, MLB1, MLB2) and clinically isolated (HAstV4, VA1) viral stocks were titrated using immunofluorescence-based detection with 8E7 (HAstV1, HAstV4) or custom polyclonal antibodies against capsid proteins (MLB1, MLB2, VA1) [8,24].

### Virus growth curves

Multistep growth curves were performed using an MOI of 0.1, with infections performed in triplicates. Equal amounts of media-derived samples were collected at 0, 24, 48, 72 and 96 hpi and titrated. The titers were determined as infectious units per ml (IU/ml).

### Electroporation of plasmid DNA

To analyze overexpressed proteins, electroporation of Huh7.5.1 cells was performed using 3 μg of plasmid DNA in complete media at 220 V and 975 μF using a Bio-Rad Gene Pulser, in the presence of 5 mM NaBes (N,N-Bis(2-hydroxyethyl)-2-aminoethanesulfonic acid sodium salt)



and 0.2 mg/ml salmon sperm carrier DNA. After electroporation, cells were split between immunofluorescent and western blotting analyses and incubated for 24 hours.

### SDS-PAGE and immunoblotting

Proteins were resolved on a 12 or 15% SDS-PAGE gel before being transferred to 0.2  $\mu$ m nitrocellulose membrane and blocked in 4% Marvel milk powder in PBS. For Bis-Tris SDS-PAGE, precast 8–16% mPAGE gels were used (Millipore) according to the manufacturer's instructions. Immunoblotting with Astrovirus 8E7 antibody (Santa Cruz Biotechnology, sc-53559, 1:1000), MLB1 anti-capsid (custom [24], 1:500), anti-HA (Abcam, ab130275, 1:3000) and anti-tubulin antibody (Abcam, ab6160, 1:1000) was followed by Licor IRDye 800 and 680 secondary antibodies (1:3000). Immunoblots were imaged on a LI-COR ODYSSEY CLx imager and analyzed using Image Studio version 5.2.

### Immunofluorescence

Infected (Figs 2–6, MOI 0.1–0.5) or electroporated (Fig 8) cells were grown on IBIDI wells, then washed with PBS and fixed with 10% formaldehyde in PHEM buffer (60 mM Pipes, 25 mM Hepes, 10 mM EGTA, 2 mM MgCl<sub>2</sub>, pH 7.0) for 15 min. Fixed cells were then washed with PBS and permeabilized with 0.1% Triton X100 or 0.1% saponin for 10 min, followed by blocking in 2% goat serum in PBS for 1 hour. For lamin staining, cells were fixed in 20% cold methanol for 15 mins. Blocked cells were stained with the following primary antibodies: MLB1/VA1 anti-capsid (1:300), Astrovirus 8E7, anti-dsRNA IgG2a (Scicons J2, 10010500, 1:250), anti-calnexin (Merck, MAB3126), anti-HA (Abcam, ab130275), anti-lamin A+C (Abcam, ab133256, 1:1000), followed by staining with Alexa 488- or 594-conjugated secondary antibody (Thermo Fisher, 1:1000). Nuclei were counter-stained with Hoechst. All confocal images are single-plane images taken with a Leica SP5 Confocal Microscope using a water-immersion 63 $\times$  objective. Image analysis was performed using JACoP plugin from ImageJ using Pearson correlation coefficient (Figs 3–6) or Manders coefficient (Fig 8).

### Proximity ligation assay

Caco2 and Huh7.5.1 cells were seeded on IBIDI wells and infected with MOI 1 for 24 hours (HAstV1 and HAstV1-HA) or MOI 0.3 for 30 hours (MLB2 and MLB2-HA). The cells were then fixed with 4% PFA for 30 minutes and permeabilized with 1% (Caco2) or 0.25% (Huh7.5.1) Triton X-100 in PBS. The cells were incubated with combinations of mouse- and rabbit-derived antibodies, followed by incubation with two PLA probes (DUO92101, Sigma Aldrich) for 1 hour at 37°C, ligation for 30 minutes, and signal amplification for another 100 minutes at 37°C. The wells were then covered with Duolink In Situ Mounting Medium with DAPI and imaged under Zeiss LSM700 microscope using an oil-immersion 63 $\times$  objective.

### Replicon assays

Linearized replicon-encoding plasmids were used to generate T7 RNAs using T7 mMACHINE mMACHINE Transcription kit (ThermoFischer, AM1344) according to the manufacturer's instructions, purified using Zymo RNA Clean & Concentrator kit and quantified. Cells were transfected in triplicate with Lipofectamine 2000 reagent (Invitrogen), using previously described reverse transfection protocol [24]. Three independent experiments, each in triplicate, were performed to confirm the reproducibility of the results.

## Protein structure prediction

The NTD 3D structure was predicted using AlphaFold 3, a neural network-based model that predicts protein three-dimensional structures from sequence, even where no similar structure is known [31–33]. The confidence of prediction was quantified by pLDDT, the predicted local distance difference test on the C $\alpha$  atoms, with >70% for most NTD regions. The alignment of two structures and amino acid residue positions were visualized using PyMOL (<https://pymol.org/>). Membrane topology was predicted using several online servers to ensure consistency.

## Statistical analyses

Data were graphed and analyzed using GraphPad Prism and MS Excel. Where appropriate, data were analyzed using one-way, two-way ANOVA, or Student's t-test test. Significance values are shown as \*\*\*\* $p < 0.0001$ , \*\*\* $p < 0.001$ , \*\* $p < 0.01$ , \* $p < 0.05$ , ns–non-significant.

## Supporting information

**S1 Data. Excel tables include all values used to generate graphs.**

(XLSX)

## Acknowledgments

We thank Jean Thompson for excellent technical assistance, the Cambridge NIHR BRC Cell Phenotyping Hub and Cambridge Advanced Imaging Centre for access to confocal microscopy. For the purpose of Open Access, the authors have applied a CC BY public copyright license to any Author Accepted Manuscript (AAM) version arising from this submission.

## Author Contributions

**Conceptualization:** Valeria Lulla.

**Formal analysis:** Hashim Ali, Jacqueline Hankinson, Aleksei Lulla, Valeria Lulla.

**Funding acquisition:** Valeria Lulla.

**Investigation:** Hashim Ali, David Noyvert, Jacqueline Hankinson, Gemma Lindsey, Valeria Lulla.

**Methodology:** Hashim Ali, David Noyvert, Jacqueline Hankinson, Gemma Lindsey, Aleksei Lulla, Valeria Lulla.

**Project administration:** Valeria Lulla.

**Resources:** Aleksei Lulla, Valeria Lulla.

**Supervision:** Hashim Ali, Valeria Lulla.

**Validation:** Aleksei Lulla.

**Visualization:** Hashim Ali, Aleksei Lulla, Valeria Lulla.

**Writing – original draft:** Hashim Ali, Valeria Lulla.

**Writing – review & editing:** Hashim Ali, David Noyvert, Jacqueline Hankinson, Aleksei Lulla, Valeria Lulla.

## References

1. Bosch A, Pintó RM, Guix S. Human astroviruses. *Clin Microbiol Rev* 2014; 27:1048–74. <https://doi.org/10.1128/CMR.00013-14> PMID: 25278582
2. Vu D-LL, Bosch A, Pintó RM, Guix S. Epidemiology of Classic and Novel Human Astrovirus: Gastroenteritis and Beyond. vol. 9. MDPI AG; 2017. <https://doi.org/10.3390/v9020033> PMID: 28218712
3. Johnson C, Hargest V, Cortez V, Meliopoulos V, Schultz-Cherry S. Astrovirus Pathogenesis. *Viruses* 2017; 9:22. <https://doi.org/10.3390/v9010022> PMID: 28117758
4. Janowski AB. Beyond the Gastrointestinal Tract: The Emerging and Diverse Tissue Tropisms of Astroviruses. *Viruses* 2021; 13. <https://doi.org/10.3390/v13050732> PMID: 33922259
5. Kawasaki J, Kojima S, Tomonaga K, Horie M. Hidden Viral Sequences in Public Sequencing Data and Warning for Future Emerging Diseases. *MBio* 2021; 12. <https://doi.org/10.1128/mBio.01638-21> PMID: 34399612
6. Finkbeiner SR, Holtz LR, Jiang Y, Rajendran P, Franz CJ, Zhao G, et al. Human stool contains a previously unrecognized diversity of novel astroviruses. *Virology* 2009; 6. <https://doi.org/10.1186/1743-422X-6-161> PMID: 19814825
7. Fuentes C, Bosch A, Pintó RM, Guix S. Identification of Human Astrovirus Genome-Linked Protein (VPg) Essential for Virus Infectivity. *J Virol* 2012; 86:10070–8. <https://doi.org/10.1128/JVI.00797-12> PMID: 22787221
8. Lulla V, Firth AE. A hidden gene in astroviruses encodes a viroporin. *Nat Commun* 2020; 11. <https://doi.org/10.1038/s41467-020-17906-x> PMID: 32792502
9. Jiang B, Monroe SS, Koonin E V, Stine SE, Glass RI. RNA sequence of astrovirus: distinctive genomic organization and a putative retrovirus-like ribosomal frameshifting signal that directs the viral replicase synthesis. *Proc Natl Acad Sci U S A* 1993; 90:10539–43. <https://doi.org/10.1073/pnas.90.22.10539> PMID: 8248142
10. Monroe SS, Jiang B, Stine SE, Koopmans M, Glass RI. Subgenomic RNA sequence of human astrovirus supports classification of Astroviridae as a new family of RNA viruses. *J Virol* 1993; 67:3611–4. <https://doi.org/10.1128/JVI.67.6.3611-3614.1993> PMID: 8497068
11. Marczinke B, Bloys AJ, Brown TD, Willcocks MM, Carter MJ, Brierley I. The human astrovirus RNA-dependent RNA polymerase coding region is expressed by ribosomal frameshifting. *J Virol* 1994; 68:5588–95. <https://doi.org/10.1128/JVI.68.9.5588-5595.1994> PMID: 8057439
12. Tao YJ, Ye Q. RNA virus replication complexes. *PLoS Pathog* 2010; 6:1–3. <https://doi.org/10.1371/journal.ppat.1000943> PMID: 20661480
13. Denison MR. Seeking membranes: positive-strand RNA virus replication complexes. *PLoS Biol* 2008; 6:2098–100. <https://doi.org/10.1371/journal.pbio.0060270> PMID: 18959488
14. Den Boon JA, Diaz A, Ahlquist P. Cytoplasmic viral replication complexes. *Cell Host Microbe* 2010; 8:77–85. <https://doi.org/10.1016/j.chom.2010.06.010> PMID: 20638644
15. Speroni S, Rohayem J, Nenci S, Bonivento D, Robel I, Barthel J, et al. Structural and biochemical analysis of human pathogenic astrovirus serine protease at 2.0 Å resolution. *J Mol Biol* 2009; 387:1137–52. <https://doi.org/10.1016/j.jmb.2009.02.044> PMID: 19249313
16. Bub T, Hargest V, Tan S, Smith M, Vazquez-Pagan A, Flerlage T, et al. Astrovirus replication is dependent on induction of double-membrane vesicles through a PI3K-dependent, LC3-independent pathway. *J Virol* 2023. <https://doi.org/10.1128/JVI.01025-23> PMID: 37668367
17. Liu Y, Wimmer E, Paul A V. Cis-acting RNA elements in human and animal plus-strand RNA viruses. *Biochim Biophys Acta* 2009; 1789:495–517. <https://doi.org/10.1016/j.bbagr.2009.09.007> PMID: 19781674
18. Walker JE, Saraste M, Runswick MJ, Gay NJ. Distantly related sequences in the alpha- and beta-subunits of ATP synthase, myosin, kinases and other ATP-requiring enzymes and a common nucleotide binding fold. *EMBO J* 1982; 1:945–51. <https://doi.org/10.1002/j.1460-2075.1982.tb01276.x> PMID: 6329717
19. Kwong AD, Rao BG, Jeang KT. Viral and cellular RNA helicases as antiviral targets. *Nat Rev Drug Discov* 2005; 4:845–53. <https://doi.org/10.1038/nrd1853> PMID: 16184083
20. Gu B, Liu C, Lin-Goerke J, Maley DR, Gutshall LL, Feltenberger CA, et al. The RNA helicase and nucleotide triphosphatase activities of the bovine viral diarrhea virus NS3 protein are essential for viral replication. *J Virol* 2000; 74:1794–800. <https://doi.org/10.1128/jvi.74.4.1794-1800.2000> PMID: 10644352
21. Xia H, Wang P, Wang GC, Yang J, Sun X, Wu W, et al. Human Enterovirus Nonstructural Protein 2CAT-Pase Functions as Both an RNA Helicase and ATP-Independent RNA Chaperone. *PLoS Pathog* 2015; 11. <https://doi.org/10.1371/journal.ppat.1005067> PMID: 26218680

22. Pfister T, Wimmer E. Characterization of the nucleoside triphosphatase activity of poliovirus protein 2C reveals a mechanism by which guanidine inhibits poliovirus replication. *J Biol Chem* 1999; 274:6992–7001. <https://doi.org/10.1074/jbc.274.11.6992> PMID: 10066753
23. Ranji A, Boris-Lawrie K. RNA helicases: emerging roles in viral replication and the host innate response. *RNA Biol* 2010; 7:775–87. <https://doi.org/10.4161/rna.7.6.14249> PMID: 21173576
24. Ali H, Lulla A, Nicholson AS, Hankinson J, Wignall-Fleming EB, Connor RLO, et al. Attenuation hotspots in neurotropic human astroviruses. *PLoS Biol* 2023; 21. <https://doi.org/10.1371/journal.pbio.3001815> PMID: 37459343
25. Hachmann JP, Amshey JW. Models of protein modification in Tris-glycine and neutral pH Bis-Tris gels during electrophoresis: effect of gel pH. *Anal Biochem* 2005; 342:237–45. <https://doi.org/10.1016/j.ab.2005.04.015> PMID: 15935323
26. den Boon JA, Nishikiori M, Zhan H, Ahlquist P. Positive-strand RNA virus genome replication organelles: structure, assembly, control. *Trends Genet* 2024. <https://doi.org/10.1016/j.tig.2024.04.003> PMID: 38724328
27. Nagy PD, Pogany J. The dependence of viral RNA replication on co-opted host factors. *Nat Rev Microbiol* 2011; 10:137–49. <https://doi.org/10.1038/nrmicro2692> PMID: 22183253
28. Puntervoll P, Linding R, Gemünd C, Chabanis-Davidson S, Mattingsdal M, Cameron S, et al. ELM server: A new resource for investigating short functional sites in modular eukaryotic proteins. *Nucleic Acids Res* 2003; 31:3625–30. <https://doi.org/10.1093/nar/gkg545> PMID: 12824381
29. Mihalič F, Simonetti L, Giudice G, Sander MR, Lindqvist R, Peters MBA, et al. Large-scale phage-based screening reveals extensive pan-viral mimicry of host short linear motifs. *Nat Commun* 2023; 14. <https://doi.org/10.1038/s41467-023-38015-5> PMID: 37100772
30. Michelsen K, Yuan H, Schwappach B. Hide and run. Arginine-based endoplasmic-reticulum-sorting motifs in the assembly of heteromultimeric membrane proteins. *EMBO Rep* 2005; 6:717–22. <https://doi.org/10.1038/sj.embor.7400480> PMID: 16065065
31. Abramson J, Adler J, Dunger J, Evans R, Green T, Pritzel A, et al. Accurate structure prediction of biomolecular interactions with AlphaFold 3. *Nature* 2024. <https://doi.org/10.1038/s41586-024-07487-w> PMID: 38718835
32. Jumper J, Evans R, Pritzel A, Green T, Figurnov M, Ronneberger O, et al. Highly accurate protein structure prediction with AlphaFold. *Nature* 2021 596:7873 2021; 596:583–9. <https://doi.org/10.1038/s41586-021-03819-2> PMID: 34265844
33. Varadi M, Anyango S, Deshpande M, Nair S, Natassia C, Yordanova G, et al. AlphaFold Protein Structure Database: massively expanding the structural coverage of protein-sequence space with high-accuracy models. *Nucleic Acids Res* 2022; 50:D439–44. <https://doi.org/10.1093/nar/gkab1061> PMID: 34791371
34. Al-Mutairy B, Walter JE, Pothen A, Mitchell DK. Genome prediction of putative genome-linked viral protein (VPg) of astroviruses. *Virus Genes* 2005; 31:21–30. <https://doi.org/10.1007/s11262-004-2196-1> PMID: 15965605
35. Murillo A, Vera-Estrella R, Barkla BJ, Méndez E, Arias CF. Identification of Host Cell Factors Associated with Astrovirus Replication in Caco-2 Cells. *J Virol* 2015; 89:10359–70. <https://doi.org/10.1128/JVI.01225-15> PMID: 26246569
36. Ravindran MS, Bagchi P, Cunningham CN, Tsai B. Opportunistic intruders: how viruses orchestrate ER functions to infect cells. *Nat Rev Microbiol* 2016; 14:407–20. <https://doi.org/10.1038/nrmicro.2016.60> PMID: 27265768
37. Guix S, Caballero S, Bosch A, Pintó RM. C-terminal nsP1a protein of human astrovirus colocalizes with the endoplasmic reticulum and viral RNA. *J Virol* 2004; 78:13627–36. <https://doi.org/10.1128/JVI.78.24.13627-13636.2004> PMID: 15564473
38. Diaz A, Wang X, Ahlquist P. Membrane-shaping host reticulon proteins play crucial roles in viral RNA replication compartment formation and function. *Proc Natl Acad Sci U S A* 2010; 107:16291–6. <https://doi.org/10.1073/pnas.1011105107> PMID: 20805477
39. Emara MM, Brinton MA. Interaction of TIA-1/TIAR with West Nile and dengue virus products in infected cells interferes with stress granule formation and processing body assembly. *Proc Natl Acad Sci U S A* 2007; 104:9041–6. <https://doi.org/10.1073/pnas.0703348104> PMID: 17502609
40. Teo CSH, Chu JH. Cellular vimentin regulates construction of dengue virus replication complexes through interaction with NS4A protein. *J Virol* 2014; 88:1897–913. <https://doi.org/10.1128/JVI.01249-13> PMID: 24284321
41. Xu K, Nagy PD. Expanding use of multi-origin subcellular membranes by positive-strand RNA viruses during replication. *Curr Opin Virol* 2014; 9:119–26. <https://doi.org/10.1016/j.coviro.2014.09.015> PMID: 25462443

42. Wolff G, Melia CE, Snijder EJ, Bárcena M. Double-Membrane Vesicles as Platforms for Viral Replication. *Trends Microbiol* 2020; 28:1022–33. <https://doi.org/10.1016/j.tim.2020.05.009> PMID: 32536523
43. Hegde RS, Keenan RJ. The mechanisms of integral membrane protein biogenesis. *Nat Rev Mol Cell Biol* 2022; 23:107–24. <https://doi.org/10.1038/s41580-021-00413-2> PMID: 34556847
44. Schutze MP, Peterson PA, Jackson MR. An N-terminal double-arginine motif maintains type II membrane proteins in the endoplasmic reticulum. *EMBO J* 1994; 13:1696–705. <https://doi.org/10.1002/j.1460-2075.1994.tb06434.x> PMID: 8157008
45. Boulaflous A, Saint-Jore-Dupas C, Herranz-Gordo MC, Pagny-Salehabadi S, Plasson C, Garidou F, et al. Cytosolic N-terminal arginine-based signals together with a luminal signal target a type II membrane protein to the plant ER. *BMC Plant Biol* 2009; 9. <https://doi.org/10.1186/1471-2229-9-144> PMID: 19995436
46. Zeyen L, Döring T, Stieler JT, Prange R. Hepatitis B subviral envelope particles use the COPII machinery for intracellular transport via selective exploitation of Sec24A and Sec23B. *Cell Microbiol* 2020; 22. <https://doi.org/10.1111/cmi.13181> PMID: 32017353
47. Li J, Fuchs S, Zhang J, Wellford S, Schuldiner M, Wang X. An unrecognized function for COPII components in recruiting the viral replication protein BMV 1a to the perinuclear ER. *J Cell Sci* 2016; 129:3597–608. <https://doi.org/10.1242/jcs.190082> PMID: 27539921
48. Aktepe TE, Liebscher S, Prier JE, Simmons CP, Mackenzie JM. The Host Protein Reticulon 3.1A Is Utilized by Flaviviruses to Facilitate Membrane Remodelling. *Cell Rep* 2017; 21:1639–54. <https://doi.org/10.1016/j.celrep.2017.10.055> PMID: 29117567
49. Chen YJ, Bagchi P, Tsai B. ER functions are exploited by viruses to support distinct stages of their life cycle. *Biochem Soc Trans* 2020; 48:2173. <https://doi.org/10.1042/BST20200395> PMID: 33119046
50. Geigenmüller U, Ginzton NH, Matsui SM. Construction of a genome-length cDNA clone for human astrovirus serotype 1 and synthesis of infectious RNA transcripts. *J Virol* 1997; 71:1713–7. <https://doi.org/10.1128/JVI.71.2.1713-1717.1997> PMID: 8995706
51. Lulla V, Dinan AM, Hosmillo M, Chaudhry Y, Sherry L, Irigoyen N, et al. An upstream protein-coding region in enteroviruses modulates virus infection in gut epithelial cells. *Nat Microbiol* 2019; 4:280–92. <https://doi.org/10.1038/s41564-018-0297-1> PMID: 30478287